Macromolecules **2006,** *39,* 9467−9472

Polymerization in Bicontinuous Microemulsion Glasses

Feng Gao, Chia-Chi Ho, and Carlos C. Co*

Department of Chemical and Materials Engineering, University of Cincinnati, 497 Rhodes Hall, Cincinnati, Ohio

Received August 14, 2006; Revised Manuscript Received September 19, 2006

ABSTRACT: Bicontinuous sugar-based microemulsions, containing up to 80 wt % of liquid divinylbenzene monomer relative to sugar, can be dehydrated to the solid glass state without phase separation. Photopolymerization of the liquid divinylbenzene present within the interstices of these solid microemulsion glass templates at temperatures below the onset glass transition of the sugar template proceeds with no phase separation. Comparison of the small angle scattering spectra of the microemulsion glasses before and after polymerization show almost no change in microstructure. Following polymerization, the bicontinuous structure of these microemulsion glasses permits straightforward and rapid dissolution of the sugar template to yield polydivinylbenzene membranes with ∼25 nm pores.

Introduction

Mixtures of water, oil, and surfactant exhibit a rich variety of microstructures, ranging from spherical micelles, rodlike micelles, and bicontinuous microemulsions to ordered liquid crystalline phases that have been extensively used as templates for the synthesis of nanomaterials.[1−15] However, with few exceptions, the structure of the final material is seldom a complementary replica of the starting template.[6,7] Identified challenges to replicating self-assembled surfactant templates, particularly with polymerization reactions, include the following: (1) overcoming changes to the interfacial curvature and equilibrium template structure as monomer is converted to polymer;[16] (2) suppressing the effects of spatially nonuniform initiation of reaction that lead to localized regions of polymer swelling and monomer depletion;[4] (3) preventing the rearrangement of the surfactant template.[17] To date, the most successful approach for replicating surfactant templates make use of polymerizable surfactants to minimize rearrangement and phase separation by "anchoring" the template to the polymerizing structure.[1,2,18−21]

We have proposed an alternative approach using solid microemulsion glasses to overcome template rearrangement during isobutyl acrylate polymerizations without the need for polymerizable surfactants.[22] Central to this approach is the replacement of water in traditional microemulsions with sugars to form solid microemulsions with bicontinuous domains of hydrophobic monomers and glassy sugar whose robust nanostructures can hold up against forces that arise during polymerization. In effect, liquid monomers are polymerized within a sugar microemulsion glass template that can easily removed by dissolution in water. Here, we examine the phase behavior of precursor microemulsions comprising of concentrated sugar solutions (>70%), divinylbenzene (DVB), and alkylglucoside surfactants that can be dehydrated to the glassy state and photopolymerized without phase separation. Unlike the poly(isobutyl acrylate)/sugar structures reported earlier that collapse upon dissolution of the sugar template,[22] cross-linked DVB/sugar microemulsions yield robust membranes with ∼25 nm pores.

Experimental Section

Materials. Technical grade C_8G_1 and $C_{12}G_1$ were supplied by Henkel (APG 225 and APG 600, respectively) in the form of 65 and 50 wt % solutions in water respectively and used as received. DVB (mixture of isomer, 80%), 1,2-octanediol, sucrose, trehalose dihydrate, and blue dextran were purchased from Aldrich and used as received. Thermally stable, UV-sensitive free-radical initiator, 2,2′-azobis(*N*-cyclohexyl-2-methylpropionamide) (Vam-111, 10 h half-life of 111 °C) was purchased from Wako Chemicals. Deionized water with a specific resistance of 18.2 MΩ cm was used.

Phase Diagram Measurements. Samples for phase behavior measurements were prepared by gently heating mixtures of sugar, water, and surfactants in flat bottom screw-cap tubes, evaporating excess water with a stream of argon, then adding octanediol and DVB. The sample tubes were immersed completely in thermostated water baths (±0.02 °C), stirred vigorously, and allowed to phase separately for up to 8 h to locate accurately the boundaries between one- and two-phase regions. 1 wt % (relative to DVB) of VAm-111 was added to samples prepared for polymerization. The presence of multiple phases was determined by visual inspection in both transmitted and scattered light, using crossed polarizers to determine the presence of liquid crystalline phases. Phase diagrams were determined to temperature and composition accuracies of ±0.2 °C and ±0.2 wt %, respectively. Following Kahlweit and Strey,[23,24] the phase space was studied by systematically varying the overall mass fraction of surfactant in the mixture (γ)

$$\gamma = \frac{\text{surfactants}}{\text{oil} + \text{sucrose} + \text{trehalose} + \text{water} + \text{surfactants} + \text{octanediol}} \tag{1}$$

and the mass fraction of DVB oil on a surfactant-free basis (α)

$$\alpha = \frac{\text{oil}}{\text{oil} + \text{sucrose} + \text{trehalose}} \tag{2}$$

With these compositional variables, α remains fixed while γ increases slightly as sugar-rich microemulsions are dehydrated to the glassy state. The phase diagrams reported here were performed holding fixed the mass ratio of C_8G_1 and $C_{12}G_1$ surfactants at 60:40 and the mass fraction of 1,2-octanediol cosurfactant in the surfactant/cosurfactant mixture at 9 wt %. Phase diagrams studying the effects of varying the ratio of C_8G_1 and $C_{12}G_1$ and the loading of octanediol cosurfactant to fine-tune the phase behavior for dehydration and template polymerization purposes are shown in

---

* Corresponding author. Telephone: (513) 556-2731. Fax: (513) 556-3473. E-mail: carlos.co@ uc.edu.

10.1021/ma061868y CCC: $33.50

Supplementary Figures 1−3. The ratio of sucrose to trehalose is fixed equimolar in all mixtures to suppress crystallization.

Preparation and Polymerization of Sugar-Based Microemulsion Glasses. Sugar-based microemulsion glasses were prepared by pouring sugar-based microemulsions into glass troughs in preequilibrated sealed chambers saturated with DVB vapor and dehydrated with anhydrous calcium sulfate at 60 °C for 8 h to form brittle, optically transparent microemulsion glasses (∼0.5 mm thick). The sealed chambers were saturated with DVB vapor and equilibrated at 60 °C (±2 °C) 1 h before use. Microemulsion glasses were photopolymerized (365 nm) at 45 °C for 72 h under argon using a 8 W UV lamp positioned 25 cm from the sample. To eliminate air-bubbles in samples for membrane permeation/selectivity testing, DVB and sugar/surfactant solutions were independently degassed and the precursor microemulsions were freeze−thawed twice before dehydration.

Modulated DSC (MDSC) Measurements. The reversible heat capacities of the microemulsion glasses were measured by modulated DSC (Q1000, TA Instruments), setting the modulation amplitude, period, and heating rate at 1 °C, 60 s, and 2 °C/min, respectively. All samples were hermetically sealed in aluminum pans during MDSC measurements, and glass transition temperatures were determined by the midpoint method.

SEM Characterization. To visualize the cross-sectional structure of the polymerized microemulsion glasses, samples were fractured at room temperature, immersed in excess water to remove the sugar template, air-dried, gold-coated, and then imaged using a scanning electron microscope (SEM, Hitachi S-900) at an accelerating voltage of 5 kV.

Small-Angle Neutron Scattering (SANS) Measurements. Small-angle neutron scattering experiments were performed using the small-angle neutron diffractometer (SAND) instrument at the Argonne National Laboratory (ANL), Argonne, IL. The scattering length density difference between sugar and divinylbenzene oil yielded acceptable coherent scattering relative to the incoherent background; thus, no deuterated compounds were used. Background correction and circular averaging was performed using software provided by ANL. Random packing of solid microemulsion glass pieces in the sample holders, however, precluded absolute intensity measurements.

Permeability and Selectivity Measurements. The permeability of the resulting membranes were measured using a 4 mm diameter syringe filter support (Corning) connected to a pressurized water reservoir maintained at 12 psi. The average thickness of the individual membranes was measured using a calibrated microscope to determine the permeability (thickness × flux/pressure drop). Triplicate measurements of membrane selectivity were performed by filtering 0.05 wt % blue dextran water solutions through the poly-DVB membranes. The filtration rate was fixed at 0.005 mL/min using a syringe pump. The sieving coefficient, defined by the ratio of blue dextran concentration in the permeate and feed streams was determined by UV.

Results and Discussion

A. Phase Behavior. Figure 1 shows the phase behavior of sugar-based microemulsions containing equal masses of sugar and DVB ($\alpha = 0.50$). Water in typical aqueous microemulsions is replaced with 70, 75, and 80 wt % sugar solutions. Above the upper phase boundary, excess oil coexists with a one-phase microemulsion, consistent with observations of microemulsion phase behavior in predominantly aqueous systems.[25−30] Phase behavior scans between the upper and lower boundaries at every composition shown in Figure 1, revealed no lamellar phases. As discussed further later, the absence of lamellar phases within this one-phase microemulsion envelope is necessary for the successful dehydration of the microemulsions to the glassy state. When cooled below the lower phase boundary, samples become increasingly birefringent and opaque and after several hours of settling, a clear oil phase is visible on top of an opaque birefringent phase. The high viscosity of the samples, and the possibility of thermally induced polymerization when samples are heated for prolonged periods thwarted efforts to check the presence of three-phase regions at lower surfactant concentrations that are typical present in aqueous microemulsion systems.[25,27−30] With increasing sugar concentration in the aqueous phase at fixed α, both the upper and lower boundaries of the one-phase microemulsion region shifts downward in temperature. Dehydration of the samples presumably removes water molecules associated with the sugar headgroups of the surfactant, biasing the interfacial curvature toward oil-continuity and therefore shifting the one-phase microemulsion region downward in temperature.[25, 27−30]

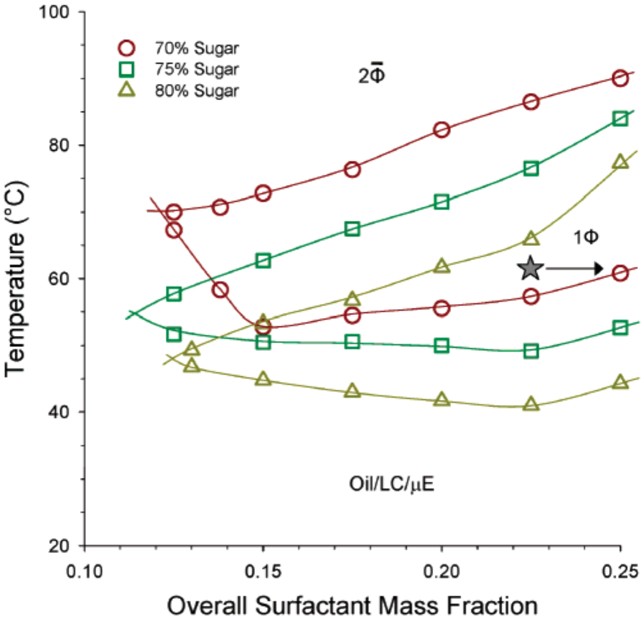

Figure 1. Phase behavior of DVB−sugar microemulsions at equal DVB to sugar mass ratio ($\alpha = 0.50$). Water in typical aqueous microemulsions is replaced with 70, 75, and 80 wt % sugar solutions equimolar in sucrose and trehalose. The star and arrow correspond to the path a microemulsion sample prepared from a 75% sugar solution takes as it is dehydrated to the glassy state without phase separation.

Consistent with earlier observations in predominantly aqueous systems with alkyl glucoside surfactants,[8,27,31] the one-phase region of these sugar-based microemulsions span a much larger temperature window than that typically observed for nonionic oligoethylene glycol surfactants[32−34] and is not interrupted by single or multiphase lamellar regions. This comparatively large one-phase microemulsion window permits controlled dehydration of the microemulsions to the glassy state without phase separation. Although the slow dynamics of microemulsions containing more than 80% sugar preclude precise phase behavior measurements, dehydration pathways, such as that marked in Figure 1, can be extrapolated that permit complete dehydration of microemulsions to the glassy state without phase separation. Practical considerations require careful tuning of the phase behavior to (1) maximize sugar loading to reduce uncertainty in the extrapolated phase behavior and (2) site the one-phase microemulsion temperature range between 45 and 75 °C, to reduce viscosity and facilitate sample transfer while avoiding premature polymerization. To satisfy these constraints, we studied the effects of varying the ratio of C_8G_1 to $C_{12}G_1$ and loading of octanediol cosurfactant in the surfactant mixture results of which are shown in Supplementary Figures 1 to 3.

Figure 2 shows the phase diagram of sugar-based microemulsions for varying DVB loading (α) on a surfactant-free

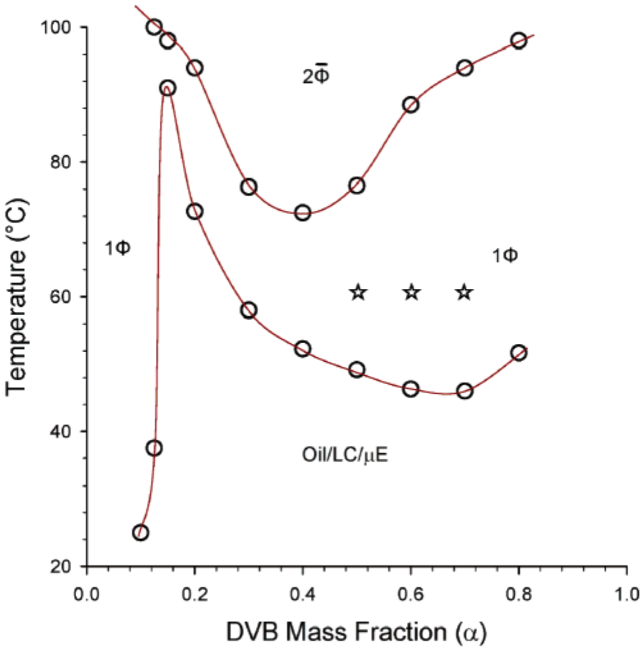

Figure 2. Effects of varying oil loading (α) on the phase behavior of DVB-sugar microemulsions. The aqueous phase is composed of a 75% sugar solution equimolar in sucrose and trehalose. Compositions and temperature at which DVB−sugar microemulsions ($\gamma = 0.225$) are dehydrated then polymerized are marked (★).

basis at a fixed overall surfactant loading (γ) of 22.5 wt %. In close analogy to the phase behavior of aqueous microemulsions prepared using alkyl−glucoside surfactants,[28] a one-phase channel spanning the whole range of oil loading is present. The compositions and temperature at which microemulsions were desiccated to the glassy state and photopolymerized are marked in Figure 2.

B. Preparation and Polymerization of DVB in Microemulsion Glasses. Sugar-based microemulsion glasses were dehydrated from mixtures of 75% sugar solution, DVB and alkyl polyglucoside (APG) at 60 °C for 8 h. After dehydration, the glasses become highly brittle but remain optically clear even after polymerization (Figure 3A). The glassy nature of these dehydrated microemulsions is evidenced in the MDSC measurements (Figure 4) that reveal distinct glass transitions. In these dehydrated microemulsions, the midpoint heating glass transition temperature shifts progressively downward from ~75 to ~64 °C as the DVB oil loading (α) increases from 0.50 to 0.80 while holding the surfactant loading fixed ($\gamma = 0.225$). With the exception of data for $\alpha = 0.60$ and 0.65, the decrease in glass transition with increasing oil loading is linear and consistent with the reduction in T_g observed for molecular liquids confined in porous silica glasses.[35] Extraction of the sugar domain size is unfortunately complicated by accompanying changes in microstructural topology with increasing oil loading which makes quantitative analysis of confinement effects by either electron microscopy or small angle scattering difficult. Dehydration of precursor liquid microemulsions containing higher DVB oil loadings ($\alpha \geq 0.85$) yields viscous liquids instead of solid glasses after dehydration. This failure to form solid percolated glass structures is not surprising however. At the maximum oil loading of $\alpha = 0.80$ where solid microemulsion glasses can be prepared by dehydration, the resulting volume fraction of liquid oil to glassy sugar is already ~6.7 to 1 because of the higher density of the sugar glass (~1500 kg/m^3) compared to divinylbenzene oil (~915 kg/m^3).

When exposed to UV light at 45 °C, the liquid DVB in the microemulsion glasses photopolymerize without macroscopic phase separation. Samples polymerized below their onset glass transition temperature remain optically clear and visually indistinguishable from unpolymerized microemulsion glasses. In contrast, samples polymerized above their glass transition become distinctly opaque. Despite the significant difference in density between DVB monomer and cross-linked poly-DVB, microstructural alterations upon polymerization of the microemulsions in their glassy state is minimal. This is evidenced by the comparable small-angle neutron scattering (SANS) spectra of the glasses before and after polymerization (Figure 5). The SANS spectra of these microemulsion glasses are in some cases, however, qualitatively different from that observed for aqueous microemulsions.

From a series expansion of a Ginzburg−Landau free-energy, Teubner and Strey developed a phenomenological scattering model for microemulsions.[36]

$$I(q) = \frac{1}{a_2 + c_1 q^2 + c_2 q^4} + b \qquad (3)$$

In this model, b accounts for background scattering while the key fitting parameters a_2, c_1, and c_2 are related to the correlation length (ξ_{TS}) and a characteristic domain size or quasi-periodic repeat distance (d_{TS}) through

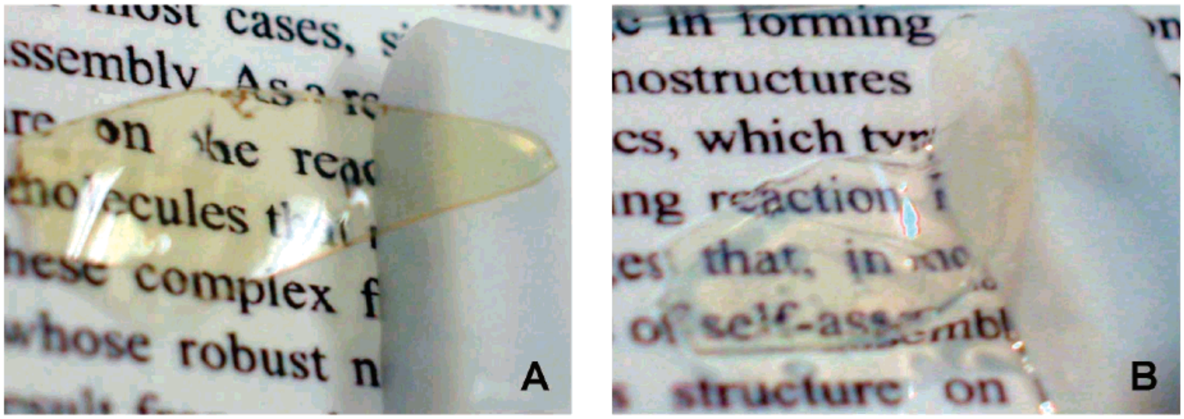

Figure 3. (A) Optically clear microemulsion glass after UV photopolymerization. (B) Dissolution of the sugar glass template with excess water leaves behind an optically clear and flexible poly-DVB membrane. The precursor microemulsion before dehydration was prepared from a 75% sugar solution with DVB oil mass loading of $\alpha = 0.60$ and overall surfactant mass loading of $\gamma = 0.225$.

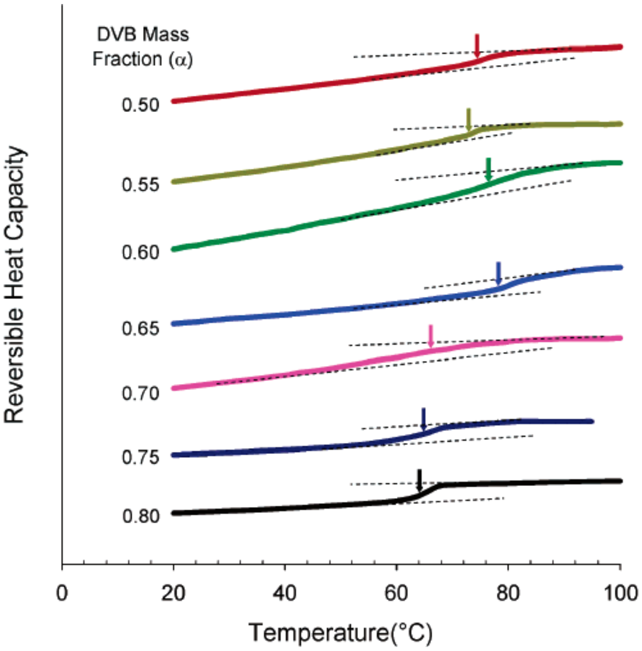

Figure 4. Modulated DSC scans of the reversible heat capacity for a series of microemulsion glasses prepared through dehydration of microemulsions prepared from a 75% sugar solution with DVB oil loading (α) ranging from 0.50 to 0.80 and overall surfactant mass loading of $\gamma = 0.225$.

$$\xi_{TS} = \left[\frac{1}{2}\left(\frac{a_2}{c_2}\right)^{1/2} + \frac{1}{4}\frac{c_1}{c_2}\right]^{-1/2} \tag{4}$$

$$d_{TS} = 2\pi\left[\frac{1}{2}\left(\frac{a_2}{c_2}\right)^{1/2} - \frac{1}{4}\frac{c_1}{c_2}\right]^{-1/2} \tag{5}$$

Model calculations of SANS spectra using the Teubner−Strey model yield an asymptotically flat profile at low-*q* with a peak at intermediate-q for structured microemulsions[37] which fit experimental scattering spectra of microemulsions well.

With the exception of microemulsion glasses prepared starting with an oil loading (α) of 0.70, the SANS spectra exhibit a progressive increase in scattering at low-*q* that is much weaker than that of phase separated samples desiccated outside the one-phase region, but nonetheless inconsistent with typical SANS spectra of liquid microemulsions. Only at higher oil-loadings (α = 0.70) does the spectra of the dehydrated microemulsion glass become comparable to that of liquid microemulsions. Analysis of the spectra at this oil loading, before and after polymerization, using the Teubner−Strey model yields domain sizes of 8.6 and 8.3 nm, respectively. In all cases, the scattering of the liquid precursor microemulsions are classical. However, the increase in viscosity during dehydration impedes diffusional relaxation of compositional gradients inevitably present in the drying samples. With increasing loading of liquid oil, the compositional and accompany microstructural gradients become locked-in at progressively later stages when the samples are almost completely dry. These gradients would explain the anomalous low-*q* scattering of the microemulsion glasses that with increasing oil loading, fade away to yield spectra consistent with the scattering from liquid microemulsions. In all cases nonetheless, the spectra of the microemulsion glasses before and after polymerization are comparable and suggestive of one-to-one templating. The slight broadening of the scattering features during polymerization appears to be unavoidable, and may be due to the inevitable increase in density following polymerization.

Key to successful dehydration and polymerization of these microemulsion glasses is the use of a temperature insensitive UV initiator to avoid premature polymerization while allowing efficient polymerization at temperatures below the onset glass transition of the sugar templates. The azo-initiator, VAm-111, which has a 10 h half-life at 111 °C is most suitable for this purpose. Radicals formed during dehydration at 60 °C for 8 h are insufficient to initiate polymerization of DVB polymerization inhibited with 1000 ppm of *p-tert*-butylcatechol. As with any photopolymerization process, matching of polymerization rate and initiator decomposition is important to form robust polymers. The intensity (distance) of the UV source (Spectroline, Westbury, NY, Model#ENF-280C, 365 nm and 8 W), was carefully adjusted at ∼25 cm, such that 5% of the initiator is decomposed (measured by UV spectroscopy) following the first 2 h of polymerization at 45 °C.

Subsequent dissolution of the sugar templates with excess water leave behind optically clear and porous poly-DVB membranes (Figure 3B) that are flexible when wet, brittle when dry, and have robust pores that resist collapse when the membranes are dried. Figure 6 shows the cross-sectional structures of porous poly-DVB membranes prepared from

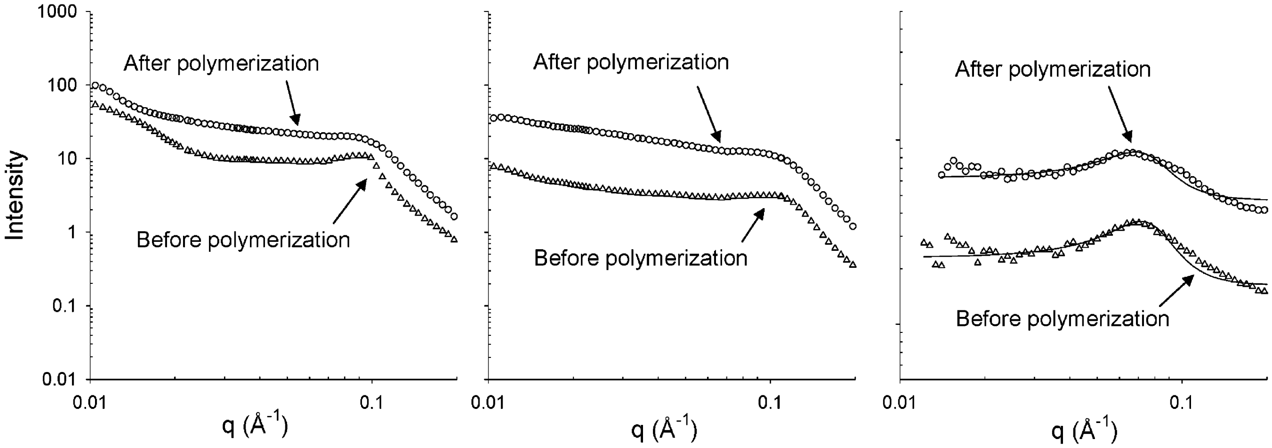

α = 0.50 α = 0.60 α = 0.70

Figure 5. SANS spectra of sugar-based microemulsion glasses before and after polymerization. Spectra are not on absolute intensity scale and were scaled for comparison. Microemulsion glass samples correspond to precursor microemulsions with initial oil to sugar mass loadings of α = 0.50, 0.60, and 0.70 as marked in Figure 2. The solid lines for α = 0.70 are model fits to the Teubner−Strey model.

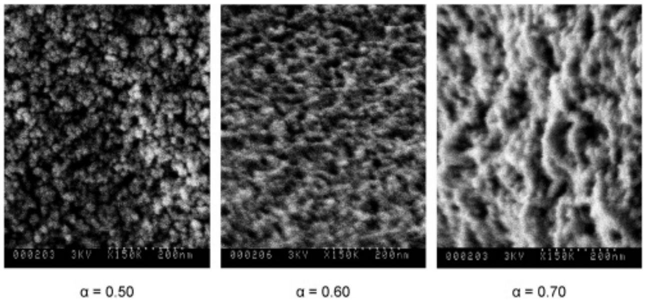

α = 0.50 α = 0.60 α = 0.70

Figure 6. Cross-sectional SEM of photopolymerized microemulsion glasses following dissolution of the sugar template with excess water. Samples were prepared from precursor liquid microemulsions with initial DVB oil loadings of $\alpha = 0.50$, 0.60, and 0.70 as marked in Figure 2.

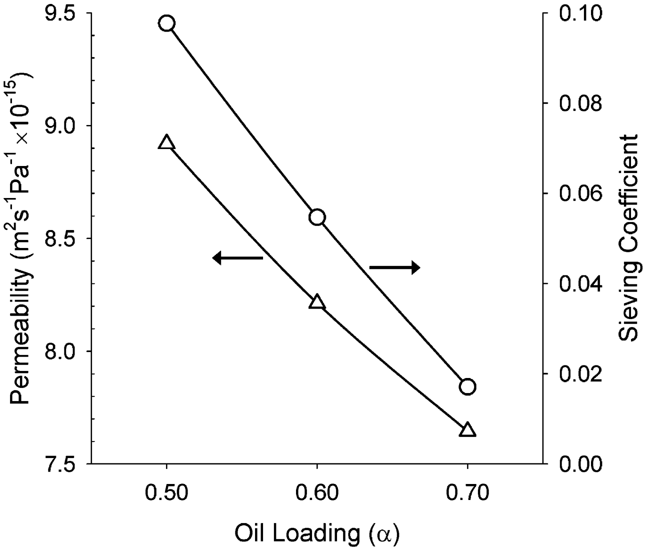

Figure 7. Permeability and sieving coefficients (2×10^6 Da dextran standard) of poly-DVB membranes prepared through dehydration, photopolymerization, and sugar template dissolution of precursor liquid microemulsions with DVB oil loading of $\alpha = 0.50$, 0.60, and 0.70 as marked in Figure 2.

precursor liquid microemulsions having DVB loadings (α) of 0.50, 0.60, and 0.70 corresponding to the compositional markers in Figure 2. Assuming minimal changes to the structures upon template removal and drying, the morphology and size of these polymer structures are comparable to the morphology of the oil domains in traditional microemulsions.[38] As expected, the decreasing porosity of the membranes with increasing oil loading (α) is reflected in the permeability and selectivity of the poly-DVB membranes (Figure 7). The sieving coefficients, measured for a 2×10^6 Da blue dextran standard, which has a radius of gyration of ~33 nm,[39] is small but finite, and overall it is consistent with the distribution of pore sizes visible in the cross-sectional images of the membranes (Figure 6).

In summary, we have demonstrated a novel approach for preparing membranes using sugar-based microemulsion glasses as templates to suppress phase separation during polymerization. These bicontinuous microemulsion glasses serve as robust templates that allow close approach to the ideal one-to-one templating limit, but can nonetheless be dissolved and potentially recycled afterward. Using sugar and sugar-based surfactants as templates eliminates the need for toxic solvents prevalent in traditional membrane manufacturing processes and is a significant advantage of this process. However, the added complexity of the dehydration and photopolymerization steps is such that this approach may be suitable only for the preparation specialty polymeric membranes for which no suitable solvents are available. The bicontinuous nature of the oil in the microemulsion glass would likely permit exchange of DVB with monomers containing functional silicon and fluorine groups for example, which do not plasticize the sugar template. This oil-exchange process would circumvent the need for extensive phase behavior studies to establish suitable dehydration pathways to the glassy state.

Conclusions

Through systematic tuning of the phase behavior of liquid sugar-rich divinylbenzene microemulsions, dehydration pathways were established to allow for their dehydration to the solid glass state without phase separation or premature polymerization. The robust microstructure of the resulting microemulsion glasses permits photopolymerization of the liquid divinylbenzene present within their interstices without phase separation. Despite the increase in density upon cross-linking of the divinylbenzene monomer, comparison of small angle scattering spectra before and after polymerization show only minimal structural rearrangement. Nonetheless, the glassy sugar template is easily removed by dissolution in excess water to yield poly(divinylbenzene) membranes with robust ~25 nm pores that resist collapse even when air-dried.

Acknowledgment. We thank Larry Rice (University of Kentucky) for assistance with the SEM imaging, Argonne National Laboratory for SAND beam time supported by Department of Energy (W-31-109-ENG-38), and the National Science Foundation (CTS#0548364) for supporting this work. The TOC graphic was adapted from Figure 1 of: Schwarz, B.; Monch, G.; Ilgenfritz, G.; Strey, R. *Langmuir* **2000**, *16*, 8643–8652.

Supporting Information Available: Supplementary Figure 1, showing phase behavior of DVB–sugar microemulsions, Supplementary Figure 2, showing effects of varying ratio of short to long alkyl chain glucoside surfactants, and Supplementary Figure 3, extent of the one-phase microemulsion channel for varying ratios of short to long alkyl chain glucoside surfactants. This material is available free of charge via the Internet at http://pubs.acs.org.

References and Notes

(1) Chew, C. H.; Li, T. D.; Gan, L. H.; Quek, C. H.; Gan, L. M. *Langmuir* **1998**, *14*, 6068–6076.
(2) Chow, P. Y.; Gan, L. M. *Adv. Polym. Sci.* **2005**, *175*, 257–298.
(3) Clapper, J. D.; Guymon, C. A. *Adv. Mater.* **2006**, *18*, 1575.
(4) Co, C. C.; de Vries, R.; Kaler, E. W. *Macromolecules* **2001**, *34*, 3224–3232.
(5) DePierro, M. A.; Guymon, C. A. *Macromolecules* **2006**, *39*, 617–626.
(6) Hentze, H. P.; Co, C. C.; McKelvey, C. A.; Kaler, E. W. *Top. Curr. Chem.* **2003**, *226*, 197–223.
(7) Hentze, H. P.; Kaler, E. W. *Curr. Opin. Colloid Interface Sci.* **2003**, *8* (2), 164–178.
(8) Kluge, K.; Stubenrauch, C.; Sottmann, T.; Strey, R. *Tenside Surfact. Det.* **2001**, *38* (1), 30–34.
(9) Lester, C. L.; Colson, C. D.; Guymon, C. A. *Macromolecules* **2001**, *34*, 4430–4438.
(10) Lester, C. L.; Guymon, C. A. *Polymer* **2002**, *43*, 3707–3715.
(11) Lester, C. L.; Smith, S. M.; Colson, C. D.; Guymon, C. A. *Chem. Mater.* **2003**, *15*, 3376–3384.
(12) McCormick, D. T.; Stovall, K. D.; Guymon, C. A. *Macromolecules* 2003, *36*, 6549–6558.
(13) Texter, J.; Ziemer, P. *Macromolecules* **2004**, *37*, 5841–5843.
(14) Yan, F.; Texter, J. *Chem. Commun.* **2006**, *25*, 2696–2698.
(15) Yan, F.; Texter, J. *Soft Matter* **2006**, *2* (2), 109–118.
(16) Eastoe, J.; Summers, M.; Heenan, R. K. *Chem. Mater.* **2000**, *12*, 3533–3537.

(17) Paul, E. J.; Prud'homme, R. K. Material synthesis by polymerization in surfactant mesophases. In *Reactions and synthesis in surfactant systems*; Texter, J., Ed.; Marcel Dekker: New York, 2001; Vol. 100, pp 525−535.

(18) Deen, G. R.; Gan, L. H.; Gan, Y. Y. *Polymer* **2004**, *45*, 5483−5490.

(19) Fu, X. A.; Qutubuddin, S. *Langmuir* **2002**, *18*, 5058−5063.

(20) Miller, S. A.; Ding, J. H.; Gin, D. L. *Curr. Opin. Colloid Interface Sci.* **1999**, *4* (5), 338−347.

(21) Summers, M.; Eastoe, J.; Davis, S.; Du, Z. P.; Richardson, R. M.; Heenan, R. K.; Steytler, D.; Grillo, I. *Langmuir* **2001**, *17*, 5388−5397.

(22) Gao, F.; Ho, C.-C.; Co, C. C. *J. Am. Chem. Soc.* **2004**, *126*, 12746−12747.

(23) Kahlweit, M.; Lessner, E.; Strey, R. *J. Phys. Chem.* **1984**, *88*, 1937−1944.

(24) Kahlweit, M.; Strey, R. *Angew. Chem., Int. Edit. Engl.* **1985**, *24*, 654−668.

(25) Ryan, L. D.; Kaler, E. W. *Colloids Surf. A* **2001**, *176* (1), 69−83.

(26) Sottmann, T.; Kluge, K.; Strey, R.; Reimer, J.; Soderman, O. *Langmuir* **2002**, *18*, 3058−3067.

(27) Reimer, J.; Soederman, O.; Sottmann, T.; Kluge, K.; Strey, R. *Langmuir* **2003**, *19*, 10692−10702.

(28) Ryan, L. D.; Kaler, E. W. *Langmuir* **1997**, *13*, 5222−5228.

(29) Ryan, L. D.; Schubert, K. V.; Kaler, E. W. *Langmuir* **1997**, *13*, 1510−1518.

(30) Ryan, L. D.; Kaler, E. W. *Langmuir* **1999**, *15*, 92−101.

(31) Reimer, J.; Soderman, O. *Langmuir* **2003**, *19*, 10692−10702.

(32) Kahlweit, M.; Strey, R.; Firman, P.; Haase, D.; Jen, J.; Schomacker, R. *Langmuir* **1988**, *4*, 499−511.

(33) Kahlweit, M.; Strey, R.; Schomacker, R.; Haase, D. *Langmuir* **1989**, *5*, 305−315.

(34) Schubert, K. V.; Kaler, E. W. *Phys. Chem. Chem. Phys.* **1996**, *100* (3), 190−205.

(35) Zhang, J.; Liu, G.; Jonas, J. *J. Phys. Chem.* **1992**, *96*, 3478−3480.

(36) Teubner, M.; Strey, R. *J. Chem. Phys.* **1987**, *87*, 3195−3200.

(37) Schubert, K. V.; Strey, R. *J. Chem. Phys.* **1991**, *95*, 8532−8545.

(38) Jahn, W.; Strey, R. *J. Phys. Chem.* **1988**, *92*, 2294−2301.

(39) Senti, F. R.; Hellman, N. N.; Ludwig, N. H.; Babcock, G. E.; Tobin, R.; Glass, C. A.; Lamberts, B. L. *J. Polym. Sci.* **1955**, *17*, 527−46.

MA061868Y